15 November 2001

ELSEVIER

Optics Communications 199 (2001) 65–75

OPTICS COMMUNICATIONS

www.elsevier.com/locate/optcom

Phase retrieval from series of images obtained by defocus variation

L.J. Allen *, M.P. Oxley

School of Physics, University of Melbourne, Parkville, Vic. 3010, Australia

Received 30 May 2001; accepted 13 September 2001

Abstract

We develop and compare three different methods of phase retrieval from series of image measurements obtained at different defocus values. The first approach is an approximate solution to the transport of intensity equation (TIE) based on Fourier transforms. The second is an exact solution of the TIE, using multigrid methods. Lastly an iterative approach, using the free space propagator between image planes, is discussed. The iterative scheme is robust in the presence of discontinuities in the phase, unlike those methods based on solution of the TIE. The performance of the different methods in the presence of noise is discussed. Application of these methods to a set of experimental images taken using X-ray imaging is investigated. A computer program which can reproduce the simulations and analyse experimental image data is briefly discussed.

Keywords: Phase retrieval; Defocus variation; Transport of intensity equation; Free space propagator; Phase discontinuities; Computer program

1. Introduction

Non-interferometric determination of the phase of quantum mechanical and classical wave fields (i.e. phase retrieval) is a topic of current interest in a number of areas where either phase imaging or structure retrieval is an issue. For example, phase measurement is topical for optical [1], X-ray [2,3], neutron [4], electron [5–8] and atom [9] wave fields. In this paper we develop and compare three different methods for phase retrieval from series of images taken at different defocus values. Firstly we consider two approaches to the solution of the transport of intensity equation (TIE), which is based on conservation of flux and has been considered, directly or indirectly, by several authors [10–14]. Here, in the first instance, we pursue an approximate solution to the TIE, starting out by making an approximation to obtain an equation of the Poisson type for an auxiliary function, as suggested by Teague [10]. We then show that, by differentiation, we can obtain a second Poisson equation for the phase itself, rather than pursuing Teague's approach based on Green functions. All the steps in this approach can be cast in terms of Fourier transforms, using well-known standard results. We note that another algorithm which starts from Teague's approximation is that proposed by Paganin and Nugent [13], which requires use of the calculus of pseudo-differential operators.

* Corresponding author. Fax: +61-3-9347-4783.
E-mail address: lja@physics.unimelb.edu.au (L.J. Allen).

0030-4018/01/$ - see front matter
PII: S0030-4018(01)01556-5

As an alternative to making any approximations, the TIE can be solved exactly using multigrid methods [15]. We implement such an approach and are thus able to compare the effect of Teague's approximation under various circumstances. Lastly we consider an iterative approach, in the spirit of Gerchberg and Saxton [16] and Misell [17], based on the use of the free space propagator between image planes [18,19]. A major advantage of this iterative scheme is that it is robust in the presence of discontinuities in the phase, unlike the methods based on solution of the TIE. The performance of the different methods in the presence of noise is discussed. Application of these methods to a set of experimental images taken using X-ray imaging is investigated. A computer program which can reproduce the simulations in this paper and can be used to analyse experimental data is briefly discussed.

2. Phase retrieval methods

The starting point for our discussion is the Schrödinger equation for the propagation of a wave in free space and in three dimensions,

$$(\nabla^2 + k^2)\Psi(\mathbf{r}) = 0, \tag{1}$$

where k is the wave number and is related to the wavelength λ of the radiation by $k = 2\pi/\lambda$. Let us assume that the wave function $\Psi(\mathbf{r})$ can be considered as a perturbation of a plane wave travelling along the z direction and can be written in the form

$$\Psi(\mathbf{r}_\perp, z) = \exp(\mathrm{i}kz)\xi(\mathbf{r}_\perp, z), \tag{2}$$

where $\mathbf{r}_\perp$ is a vector in the x–y plane and perpendicular to the z direction. Then with the paraxial approximation that the second partial derivative of $\xi(\mathbf{r}_\perp, z)$ with respect to z is small, i.e. $\partial_z^2\xi(\mathbf{r}_\perp, z) \approx 0$, we obtain

$$(\nabla_\perp^2 + 2\mathrm{i}k\partial_z)\xi(\mathbf{r}_\perp, z) = 0, \tag{3}$$

where $\nabla_\perp$ operates in the x–y plane.

Writing the wave function in Eq. (3) terms of an intensity I and phase ϕ as

$$\xi(\mathbf{r}_\perp, z) = I^{1/2}(\mathbf{r}_\perp, z)\exp[\mathrm{i}\phi(\mathbf{r}_\perp, z)], \tag{4}$$

we can obtain the following equation for the phase, which expresses conservation of flux in a paraxial approximation and which is often referred to as the TIE [10]:

$$\nabla_\perp \cdot [I(\mathbf{r}_\perp, z)\nabla_\perp\phi(\mathbf{r}_\perp, z)] = -k\partial_z I(\mathbf{r}_\perp, z). \tag{5}$$

The term $\partial_z I(\mathbf{r}_\perp, z)$ is the intensity derivative along the direction of propagation at an image plane defined by the variable $\mathbf{r}_\perp$ for a given value of z. Given $I(\mathbf{r}_\perp, z)$ and $\partial_z I(\mathbf{r}_\perp, z)$ as data, and assuming continuity of the phase $\phi(\mathbf{r}_\perp, z)$, this equation has a unique solution for the phase provided that $I(\mathbf{r}_\perp, z) > 0$ everywhere in the image plane [20]. If there are points where $I(\mathbf{r}_\perp, z) = 0$ (which indicates the possible presence of vortices in the phase map) then phase retrieval using Eq. (5) will not yield unique results in general [19]. We now consider different methods by which phase retrieval may be achieved.

2.1. Approximate phase retrieval using the TIE

An approach to obtain an approximate solution to Eq. (5) was proposed by Teague [10]. This approach is based upon Helmoltz's theorem [21] by which one can decompose the vector field $I(\mathbf{r}_\perp, z)\nabla_\perp\phi(\mathbf{r}_\perp, z)$ in Eq. (5) as

$$I(\mathbf{r}_\perp, z)\nabla_\perp\phi(\mathbf{r}_\perp, z) = \nabla_\perp\psi(\mathbf{r}_\perp, z) + [\nabla \times \mathbf{A}(\mathbf{r}_\perp, z)]_\perp, \tag{6}$$

where $\psi(\mathbf{r}_\perp, z)$ is a continuous scalar field and $\mathbf{A}(\mathbf{r}_\perp, z)$ is a vector potential (which without loss of generality may be assumed to be divergence free). In Teague's approximation the rotational term $[\nabla \times \mathbf{A}(\mathbf{r}_\perp, z)]_\perp$ is ignored so that Eq. (5) reduces to one of the Poisson type for the auxiliary function $\psi(\mathbf{r}_\perp, z)$,

$$\nabla_\perp^2\psi(\mathbf{r}_\perp, z) = -k\partial_z I(\mathbf{r}_\perp, z). \tag{7}$$

Teague has then suggested a Green function approach to determine the phase. We propose to obtain the phase using a different approach. We start with the standard formula for the Fourier transform (denoted by $\mathscr{F}$) of the nth partial derivative of the function $f(x, y)$ with respect to x:

$$\mathscr{F}\left[\partial_x^{(n)} f(x, y)\right] = \mathrm{i}^n q_x^n \mathscr{F}[f(x, y)]. \tag{8}$$

Here q_x is the variable conjugate to x in the Fourier space. Eq. (8) follows, for example, from formula 33.20 in Ref. [22]. A similar equation applies to partial differentiation with respect to y. This means that we can write

$$\nabla_\perp f(x,y) = \mathrm{i}\hat{\mathbf{x}}\mathscr{F}^{-1}q_x\mathscr{F}[f(x,y)] + \mathrm{i}\hat{\mathbf{y}}\mathscr{F}^{-1}q_y\mathscr{F}[f(x,y)], \tag{9}$$

where $\hat{\mathbf{x}}$ and $\hat{\mathbf{y}}$ are unit vectors in the x and y directions respectively. It follows from Eq. (9) that

$$\nabla_\perp^2 f(x,y) = -\mathscr{F}^{-1}\left(q_x^2+q_y^2\right)\mathscr{F}[f(x,y)] \equiv -\mathscr{F}^{-1}q_\perp^2\mathscr{F}[f(x,y)], \tag{10}$$

where $q_\perp$ is the magnitude of the variable conjugate to $\mathbf{r}_\perp$ in the Fourier space. Using Eq. (10) it follows that the solution of Eq. (7) is given by

$$\psi(\mathbf{r}_\perp,z) = \mathscr{F}^{-1}q_\perp^{-2}\mathscr{F}[k\partial_z I(\mathbf{r}_\perp,z)]. \tag{11}$$

Using Eq. (9) twice it is then easy to construct the quantity $\nabla_\perp\cdot[I^{-1}(\mathbf{r}_\perp,z)\nabla_\perp\psi(\mathbf{r}_\perp,z)]$ which, from Eq. (6) with the rotational term once again discarded, is just the right hand side of a second Poisson equation, this time for the phase $\phi(\mathbf{r}_\perp,z)$:

$$\nabla_\perp^2\phi(\mathbf{r}_\perp,z) = \nabla_\perp\cdot\left[I^{-1}(\mathbf{r}_\perp,z)\nabla_\perp\psi(\mathbf{r}_\perp,z)\right]. \tag{12}$$

Then using Eq. (10) again we can solve for the phase: $\phi(\mathbf{r}_\perp,z)$

$$\phi(\mathbf{r}_\perp,z) = -\mathscr{F}^{-1}q_\perp^{-2}\mathscr{F}\left\{\nabla_\perp\cdot\left[I^{-1}(\mathbf{r}_\perp,z)\nabla_\perp\psi(\mathbf{r}_\perp,z)\right]\right\}. \tag{13}$$

An implicit assumption in the solution for the phase is that it satisfies periodic boundary conditions. Due to the division by the intensity $I(\mathbf{r}_\perp,z)$ it is necessary to ensure stable numerical evaluation of Eq. (12). This may be achieved by specifying a cut-off parameter α and setting $I(\mathbf{r}_\perp,z)_{\text{cut-off}} = \alpha I(\mathbf{r}_\perp,z)_{\max}$, where $I(\mathbf{r}_\perp,z)_{\max}$ is the maximum value of the intensity in the principal (central) plane. If $I(\mathbf{r}_\perp,z)\leqslant I(\mathbf{r}_\perp,z)_{\text{cut-off}}$ then $I(\mathbf{r}_\perp,z)$ is set to $I(\mathbf{r}_\perp,z)_{\text{cut-off}}$ when evaluating the term in square brackets in Eq. (12). For similar reasons values of $q_\perp = 0$ must be treated with care when evaluating Eqs. (11) and (13).

It can be shown that the outcome of the chain of reasoning in this section is a series of operations which yield an equivalent solution for the phase to that expressed in terms of pseudo-differential operators in Eq. (21) in Ref. [13].

2.2. Exact phase retrieval using the TIE

We can rewrite the TIE, given by Eq. (5), in the form

$$I(\mathbf{r}_\perp,z)\partial_x^2\phi(\mathbf{r}_\perp,z) + I(\mathbf{r}_\perp,z)\partial_y^2\phi(\mathbf{r}_\perp,z) + \partial_x I(\mathbf{r}_\perp,z)\times\partial_x\phi(\mathbf{r}_\perp,z) + \partial_y I(\mathbf{r}_\perp,z)\partial_y\phi(\mathbf{r}_\perp,z) = -k\partial_z I(\mathbf{r}_\perp,z), \tag{14}$$

which reveals its structure as a linear, two-dimensional, non-separable and elliptic partial differential equation of the second kind. This equation has a unique solution provided that $I(\mathbf{r}_\perp,z) > 0$ in the solution region. We can solve for $\phi(\mathbf{r}_\perp,z)$ on a given rectangular region using multigrid methods [15], as implemented, for example, in the subroutine mud2 in the suite of programs MUDPACK 5.0, written by Adams [23,24] and which can be found at the web site http://www.scd.ucar.edu/css/software/mudpack. The boundary conditions on the edges of the rectangle must be specified. Since these are not known a priori the best that can be done in practice is to assume that the phase $\phi(\mathbf{r}_\perp,z)$ is periodic and, in addition, has some specified constant value c on the boundaries. It is necessary to specify c, otherwise, with only periodicity assumed, the partial differential equation is singular and mud2 fails. Since $\phi(\mathbf{r}_\perp,z)$ is only determined up to an arbitrary overall constant, the constant c can be chosen arbitrarily. A method to solve Eq. (5) exactly has also been proposed by Van Dyck and Coene [25], but it requires considerable computational resources. That method finds the Fourier coefficients of the phase $\phi(\mathbf{r}_\perp,z)$, although only a subset are retrieved in practice.

2.3. Exact phase retrieval using an iterative approach

The solution of Eq. (3) can formally be written as [10]

$$\xi(\mathbf{r}_\perp,z=\Delta z) = \exp\left(\frac{\mathrm{i}\Delta z}{2k}\nabla_\perp^2\right)\xi(\mathbf{r}_\perp,z=0). \tag{15}$$

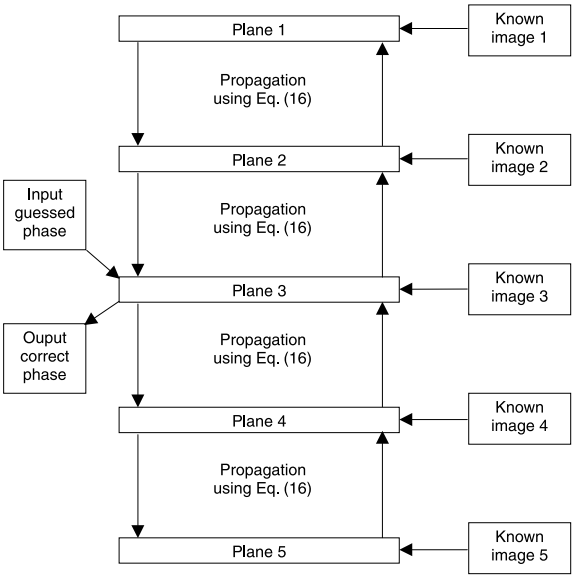

Fig. 1. Schematic diagram of the iterative method of phase retrieval discussed in Section 2.3.

Using Eq. (8) again we may show that

$$\xi(\mathbf{r}_\perp, z = \Delta z) = \mathscr{F}^{-1} \exp\left(-\frac{\mathrm{i}\Delta z q_\perp^2}{2k} \right) \mathscr{F}[\xi(\mathbf{r}_\perp, z = 0)], \tag{16}$$

which describes the free space propagation of the wave function from the plane at $z = 0$ to that at $z = \Delta z$.

The iterative phase retrieval method used in this paper is shown schematically in Fig. 1. We start at the principal (central) Plane 3 and construct a wave function via Eq. (4) from the intensity of the known image and a guess for the phase map (in practice zero everywhere). We then propagate this wave function to Plane 4 using Eq. (16). Unless our initial guess for the phase is correct, the intensity of the propagated wave function will not agree with that of the known image at Plane 4. We replace the intensity of the propagated wave function with the known values. We then propagate to Plane 5, where the intensity is again corrected to the known values. We then back-propagate to Plane 4 and continue in a cycle, encompassing Planes 1 and 2, back to Plane 3 (as indicated by the arrows). After a complete cycle we check the sum squared error (SSE) [26] of the predicted intensity relative to the known image intensity in the principal plane. We continue iterating until either a convergence criterion, defined in terms of the SSE, is satisfied or the SSE no longer decreases and stagnation occurs. Various iterative phase methods and their performance have been discussed previously [26,27]. Stagnation problems and their solution have been investigated [28] and issues of uniqueness have also been explored [19,29]. We have found that the approach described here converges reliably from a starting guess of a constant phase for a wide variety of test cases—provided that the images are sufficiently far apart that there are substantial differences between the images in the series [19]. We note that the iterative method retrieves phase correctly in the case of vortices or edge dislocations in the phase [19,30].

The iterative methods require sampling at a higher rate than do the methods based on the TIE. The formation of the wave function at each step means that the oscillatory functions $\sin(\phi)$ and $\cos(\phi)$ must be accurately evaluated, whereas the TIE is directly an equation whose solution is the phase. Therefore, caution is required when rapid variations are expected in the recovered phase. If suitable data is available, checking with one of the TIE methods is one possible strategy. However, an advantage of the iterative method of phase retrieval is that there is no need to assume that the phase satisfies periodic boundary conditions, as is the case when solving the TIE.

3. Comparison of performance of phase retrieval methods

3.1. Model solutions of the phase problem for pseudo-data

To investigate the performance of the phase retrieval methods discussed in the previous section we have started from the following model image and phase maps (assumed to be at zero defocus). The image is given by

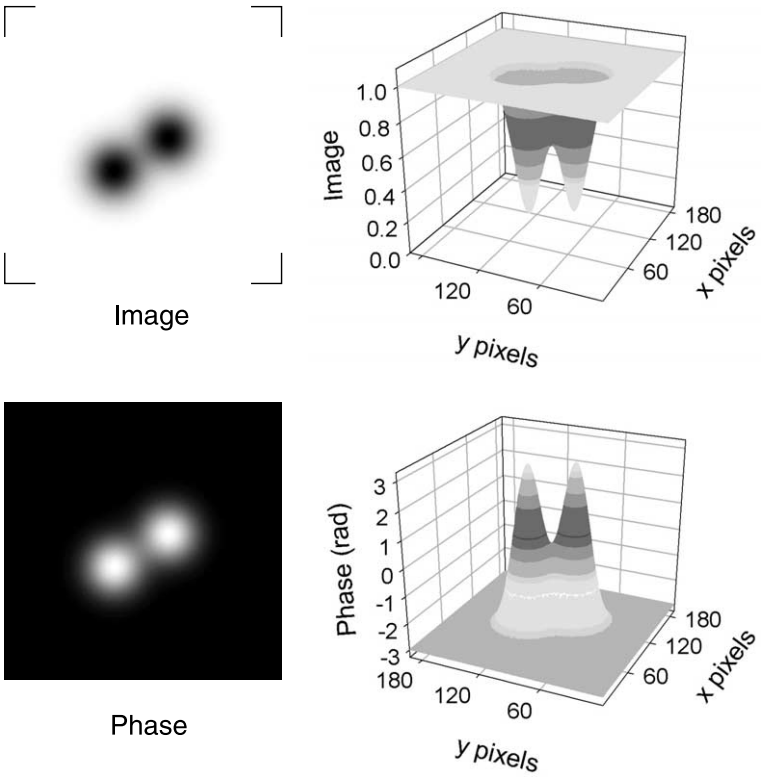

Fig. 2. Input model image and phase given by Eqs. (17) and (18) (assumed to be at zero defocus) and shown as both grey scale and surface plots.

$$I(x,y) = 1.0 - 0.9\Big(\exp\Big\{-b^2\Big[(x-x_1)^2 + (y-y_1)^2\Big]\Big\} + \exp\Big\{-b^2\Big[(x-x_2)^2 + (y-y_2)^2\Big]\Big\}\Big), \tag{17}$$

where $b = 0.0027$. The location of the centre of the first Gaussian peak is at (x_1, y_1) with $x_1 = 2n_x/5$ and $y_1 = 3n_y/5$ and n_x and n_y are the numbers of pixels along the x and y directions respectively. The second Gaussian is centred at (x_2, y_2) with $x_2 = 3n_x/5$ and $y_2 = 2n_y/5$. The phase almost covers the range between $-\pi$ and π and is given by

$$\phi(x,y) = 0.95\left\{\frac{2\pi}{0.9}[1.0 - I(x,y)] - \pi\right\}. \tag{18}$$

The factor of 0.95 is to avoid phase wrapping due to numerical rounding in our calculations. The image and phase given by Eqs. (17) and (18) are shown in Fig. 2, both as grey scale plots and as surface plots. The pictures have a resolution of 193×193 pixels. This number was chosen to facilitate the use of mud2, which requires certain pixel numbers to operate (this can be accommodated by appropriate padding in general). It should also be noted that this number of pixels is a worst case scenario in terms of speed of execution for the approximate solution of the TIE and the iterative method since the Fourier transforms are slow as opposed to fast transforms (which require the number of pixels to be multiples of small primes [15]). Nevertheless to ensure a rigorous comparison, all simulations are done with this number of pixels.

Let as assume that the image in Fig. 2 is of an object 1×1 mm^2 and is formed using incident

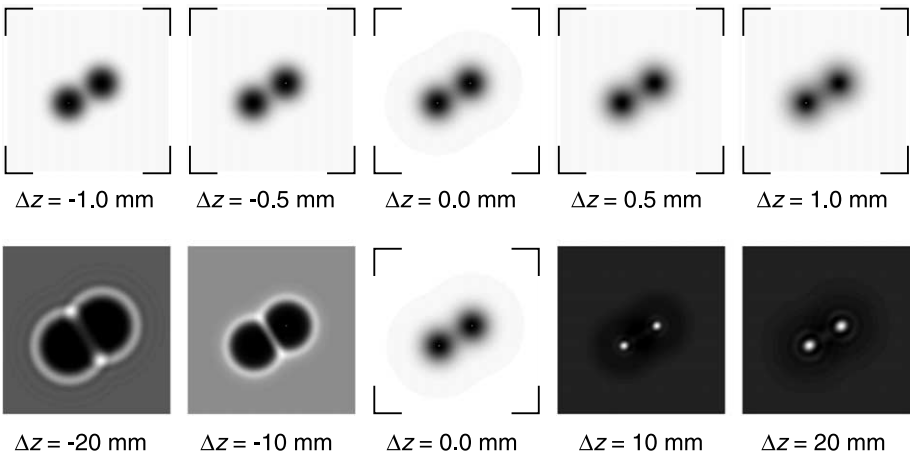

Fig. 3. Two through focal series about zero defocus with step sizes in the defocus of $\delta z = 0.5$ and 10 mm respectively.

radiation of wavelength 6328 Å (HeNe laser). Using the free space propagator given by Eq. (16), series of images with different defocus can be calculated that are suitable for testing and comparing the different phase retrieval methods. The first series shown in Fig. 3, with a step size in the defocus of $\delta z = 0.5$ mm between images, is suitable for phase retrieval in the plane $\Delta z = 0$ mm using either the Fourier or multigrid methods of phase retrieval using the TIE (where an estimate needs to be made of the quantity $\partial_z I(\mathbf{r}_\perp, z)$). The second series of images has a larger difference in defocus of $\delta z = 10$ mm and is suitable for use with the iterative method of phase retrieval. Note that we use Δz to refer to the defocus value of a principle image (in the plane of which we wish to retrieve the phase) and δz to refer to the step size used to generate the series of images used in the phase retrieval at that principle value. Consistent with Eqs. (15) and (16), we use the convention that Δz is positive for underfocus. For example in this convention the Scherzer defocus is a positive quantity. Shown in the first row in Fig. 4 is the image and phase in the plane $\Delta z = 0$ and the phase obtained using the three methods of phase retrieval from the pertinent series of images that are shown in Fig. 3. All three methods perform well in this case. The minimum and maximum values of the input and recovered phase maps are shown beneath them (in radians) and each of the grey scale plots is scaled between these values.

Subsequent lines of results in Fig. 4 were obtained by taking the image and phase shown for a given defocus value and generating a series of images about that principal image in the same way as shown in Fig. 3 for $\Delta z = 0$ mm. This means a step size $\delta z = 0.5$ mm was used to generate the images for use with the TIE methods while $\delta z = 10$ mm was used to generate the series of images for use with the iterative phase retrieval method. Phase retrieval was then attempted using each method. An important point to notice is the case where the principal image has $\Delta z = -20$ mm. Here two pairs of vortices have developed in the phase and each pair is joined by a branch cut. One vortex is indicated by an arrow in the input phase map in the last row in Fig. 4. This vortex behaviour is preceded by increasing rotation in the vector field $I(\mathbf{r}_\perp, z)\nabla_\perp \phi(\mathbf{r}_\perp, z)$, so that neglect of the possible vector potential in Eq. (6), as done by Teague [10], means that the Fourier transform approach to the phase retrieval performs less and less satisfactorily as the vortex behaviour in the phase is approached. The multigrid method on the other hand gives reasonable results until the vortex is reached, at which point it also fails. The iterative method retrieves the phase correctly in all cases and in particular in the presence of vortices.

The phase maps in Fig. 4 are all shown wrapped into the interval $[-\pi, \pi]$, since unwrapping phase maps in the presence of a singularity is not straightforward.

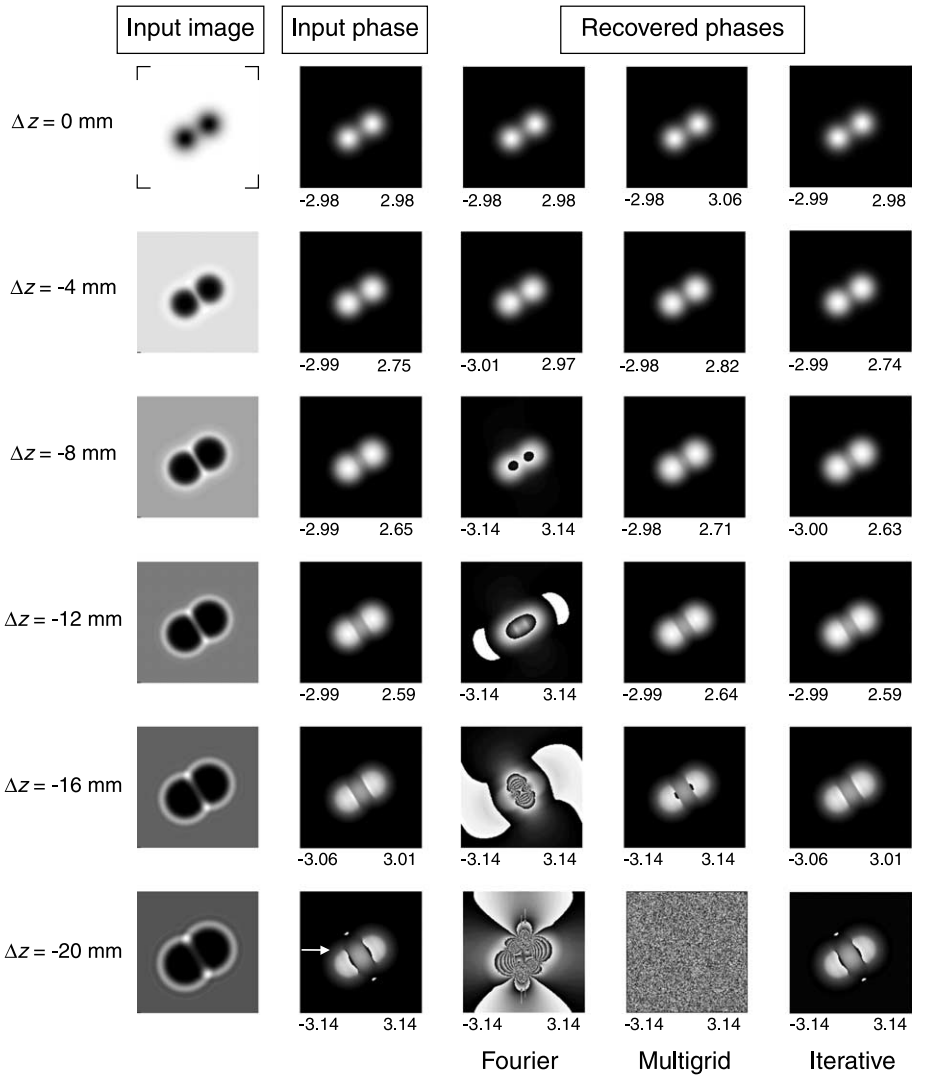

Fig. 4. Performance of phase retrieval methods for the input principal wave functions shown in the first two columns. The wave functions were obtained by propagating the wave function in Fig. 2 in free space to the defocus values indicated. Through focal series were then constructed about each of these principal wave functions, as explained in the text. Minimum and maximum values are indicated below each phase map (in radians) and each is scaled to its own minimum and maximum. The phase maps are all shown wrapped into the interval $[-\pi, \pi]$.

3.2. Model solutions for pseudo-data in the presence of noise

Simulations were also run with noise in the images for the focus series generated about $\Delta z = 0$ mm. We assigned a number of counts to each pixel assuming that the maximum intensity in the principal (central) image corresponded to 400 or 100 counts. This corresponds to noise at the 5% and 10% level respectively for maximum intensity (with larger errors, of course, at all other pixels). The statistical errors at each pixel were assigned using a random deviate drawn from a Poisson distribution with mean corresponding to the noise-free number of counts for a given pixel [15].

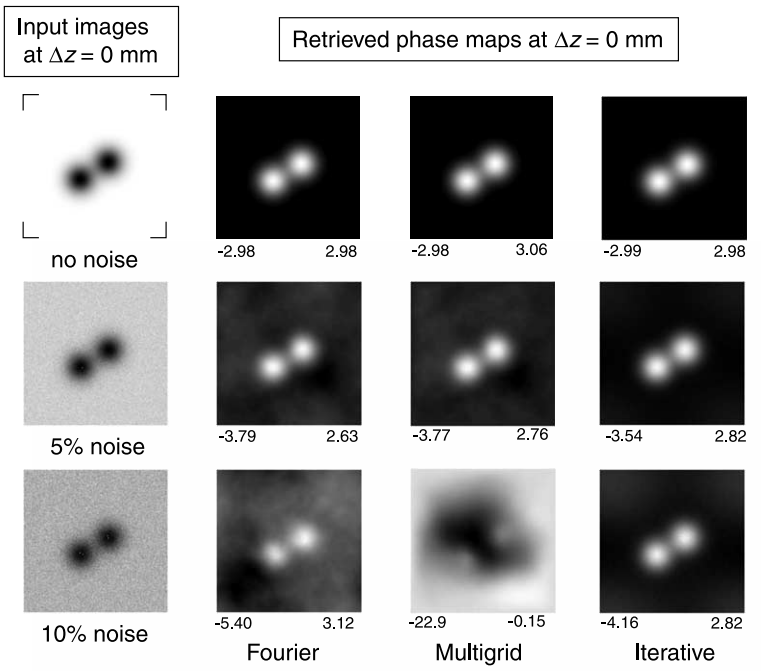

Fig. 5. The effect of noise on the performance of the phase retrieval methods discussed in this paper is shown by comparing phase maps recovered in the presence of 5% and 10% noise with those recovered in the absence of noise.

With a noise level of 5% on the brightest pixel, all methods still gave reasonable results, as can be seen in Fig. 5. The phases are shown unwrapped and the maximum and minimum value of the phase is indicated below each map. However at the 10% level the multigrid method failed. The Fourier result is better but the Gaussian peaks are no longer of equal height, while the iterative approach delivered the best result. The iterative method achieved an SSE of 1.1×10^{-3} for the data with 5% noise and 4.2×10^{-2} for that with 10% noise. The approaches solving the TIE are more sensitive to noise due to the small steps in defocus required to estimate the intensity change along the z direction. Further sources of error have been discussed by Misell [31].

3.3. Phase retrieval from experiment

Fig. 6 shows a series of experimental images provided for test purposes by Dr. McMahon. The images, of a silicon tip from an atomic force microscope (AFM), were formed using X-rays of energy 1.83 keV (wavelength 6.78 Å) and a zone plate at the Argonne National Laboratory in USA. Further discussion of the methods employed can be found in Ref. [32], where non-interferometric quantitative phase imaging with soft X-rays was demonstrated. Care was taken in aligning the images, which before padding were 70×70 pixels and represent a physical image size of 1.69×1.69 mm^2. The images were separated by a free space propagation distance of 26.9 m. We padded the images by their average value on the boundary to 97×97 pixels. Padding to this size facilitates use of the multigrid routine mud2 and provides the periodic boundary conditions that both approaches to the solution of the TIE assume. The recovered phase images are shown in Fig. 6. More high frequency detail is evident in the phase map for the iterative method and is consistent with the noisy background evident in the input images.

3.4. Computer program

A computer program, PhaseRetrieval, which will run under Windows 32-bit operating systems

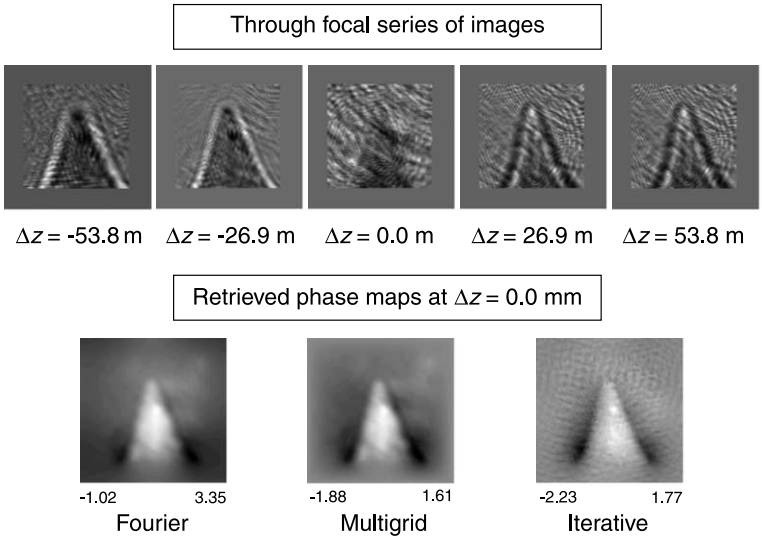

Fig. 6. Phase retrieval from a through focal series of X-ray images of a silicon tip from an AFM. The X-rays had an energy of 1.83 keV ($\lambda = 6.77$ Å). Each image, originally 70×70 pixels, representing a linear size of 1.69 mm, has been padded with its average value on the boundary to 97×97 pixels.

and which incorporates all three approaches to the phase retrieval discussed in this paper, is available for academic, non-commercial purposes by e-mailing the authors. It will reproduce the simulations presented in this paper. In addition it has the facility to do phase retrieval from experimental images up to 513×513 pixels in size (including any padding). It requires two, three or five experimental images in equally spaced planes. The use of more than two images with the iterative approach is wise. Then one covers the possibility of discontinuities, and in particular vortices, in the phase of the wave function in one or more of the planes [19]. The iterative method is set to continue iterating until either the SSE reaches 10^{-15} (usually only achieved with simulated data with no noise added) or stagnation occurs (the SSE does not reduce for 30 iterations) or it is terminated by the user.

A screen shot of PhaseRetrieval on completion of the phase retrieval from a more complicated series of simulated images than we have considered here is shown in Fig. 7.

Images (and phases for simulations) can be input and output in two formats, a grid format and in text image format used, for example by the image processing software ImageJ written by Wayne Rasband. ImageJ is in the public domain and can be downloaded from http://rsb.info.nih.gov/ij/download.html. Caution needs to be exercised in converting images in other formats to text image format, where they will be scaled between 0 and 255 (256-level grey scale) and the relative intensity between different images may be lost. A renormalization, based upon conservation of flux, may be required.

4. Summary and conclusions

We have developed and compared the use of three different methods of phase retrieval from series of image measurements obtained at different defocus values. The first approach was an approximate solution to the TIE based on Fourier transforms. The second method was an exact solution of the TIE using multigrid methods. Finally an iterative approach using the free space propagator between image planes was discussed. The approximate solution of the TIE was adequate in circumstances where the phase was continuous and the rotational component of the vector field

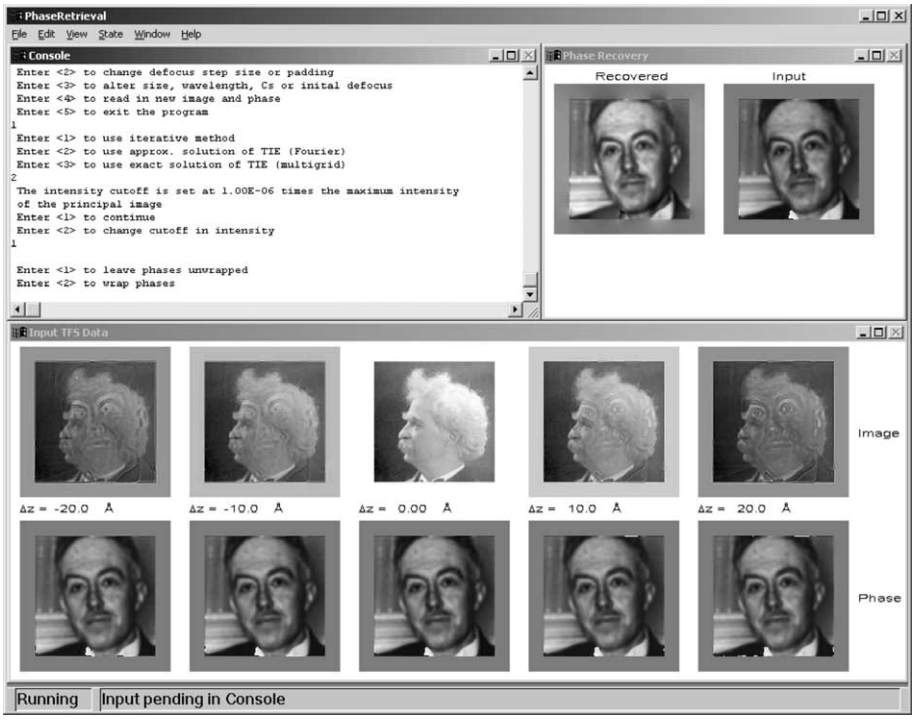

Fig. 7. Screen shot of the computer program discussed in the text after retrieving the phase of a model wave function consisting of Mark Twain as the image and Louis–Victor de Broglie as the phase.

$I(\mathbf{r}_\perp, z)\nabla_\perp\phi(\mathbf{r}_\perp, z)$ was small. The latter restriction is removed if the TIE is solved exactly using multigrid methods. The iterative scheme is robust in the presence of discontinuities in the phase, unlike the methods based on solution of the TIE. The performance of the different methods in the presence of noise was discussed, the iterative method being the most robust. Application of these methods to a set of experimental images taken using X-ray imaging was demonstrated. In general the iterative method performs better than those based on the TIE. A computer program which can reproduce the simulations and analyse experimental image data was briefly discussed.

Acknowledgements

The authors would like to thank, Dr. K. Amos, H.M.L. Faulkner, Dr. P.J. McMahon, Prof. K.A. Nugent, Dr. D. Paganin and Prof. H. von Geramb for stimulating and useful discussions. We are particularly grateful to Dr. P.J. McMahon for providing the experimental X-ray images. L.J.A. acknowledges financial support from the Australian Research Council.

References

[1] A. Barty, K.A. Nugent, D. Paganin, A. Roberts, Opt. Lett. 23 (1998) 817–819.
[2] K.A. Nugent, T.E. Gureyev, D. Cookson, D. Paganin, Z. Barnea, Phys. Rev. Lett. 77 (1996) 2961–2964.
[3] T.E. Gureyev, C. Raven, A. Snigirev, I. Snigireva, S.W. Wilkins, J. Phys. D: Appl. Phys. 32 (1999) 563–567.
[4] B.E. Allman, P.J. McMahon, K.A. Nugent, D. Paganin, D.L. Jacobson, M. Arif, S.A. Werner, Nature 408 (2000) 158–159.
[5] A. Tonomura, Physica B 280 (2000) 227–228.
[6] S. Bajt, A. Barty, K.A. Nugent, M. McCartney, M. Wall, D. Paganin, Ultramicroscopy 83 (2000) 67–73.
[7] J.C.H. Spence, Acta Cryst. A 54 (1998) 7–18.
[8] L.J. Allen, H.M.L. Faulkner, H. Leeb, Acta Cryst. A 56 (2000) 119–126.

[9] K.A. Nugent, D. Paganin, Phys. Rev. A 61 (2000) 063614–1–063622–9.
[10] M.R. Teague, J. Opt. Soc. Am. 73 (1983) 1434–1441.
[11] F. Roddier, C. Roddier, Appl. Opt. 30 (1991) 1325–1327.
[12] C. Roddier, F. Roddier, J. Opt. Soc. Am. A 10 (1993) 2277–2287.
[13] D. Paganin, K.A. Nugent, Phys. Rev. Lett. 80 (1998) 2586–2589.
[14] P.M. Blanchard, D.J. Fisher, S.C. Woods, A.H. Greenaway, Appl. Opt. 39 (2000) 6649–6655.
[15] W.H. Press, S.A. Teukolsky, W.T. Vetterling, B.P. Flannery, Numerical Recipes in Fortran, second ed., Cambridge University Press, Cambridge, 1992.
[16] R.W. Gerchberg, W.O. Saxton, Optik 35 (1972) 237–246.
[17] D.L. Misell, J. Phys. D: Appl. Phys. 6 (1973) 2200–2216.
[18] L.J. Allen, H.M.L. Faulkner, M.P. Oxley, D. Paganin, Ultramicroscopy 88 (2001) 85–97.
[19] L.J. Allen, H.M.L. Faulkner, K.A. Nugent, M.P. Oxley, D. Paganin, Phys. Rev. E 63 (2001) 037602–1–037602–4.
[20] T.E. Gureyev, A. Roberts, K.A. Nugent, J. Opt. Soc. Am. A 12 (1995) 1942–1946.
[21] P.M. Morse, H. Feshbach, Methods of Theoretical Physics, Part I, McGraw-Hill, New York, 1953.
[22] M.R. Spiegel, Mathematical Handbook of Formulas and Tables, McGraw-Hill, New York, 1968.
[23] J. Adams, Appl. Math. Comp. 34 (1989) 113–146.
[24] J. Adams, Appl. Math. Comp. 53 (1993) 235–249.
[25] D. Van Dyck, W. Coene, Optik 77 (1987) 125–128.
[26] W.O. Saxton, Computer Techniques for Image Processing in Electron Microscopy, Academic Press, New York, 1978.
[27] J.R. Fienup, Appl. Opt. 21 (1982) 2758–2769.
[28] J.R. Fienup, C.C. Wackerman, J. Opt. Soc. Am. A 3 (1986) 1897–1907.
[29] J.H. Seldin, J.R. Fienup, J. Opt. Soc. Am. A 7 (1990) 412–427.
[30] L.J. Allen, M.P. Oxley, Ultramicroscopy 88 (2001) 195–209.
[31] D.L. Misell, J. Phys. D: Appl. Phys. 6 (1973) 2217–2225.
[32] B.E. Allman, P.J. McMahon, J.B. Tiller, K.A. Nugent, D. Paganin, A. Barty, I. McNulty, S.P. Frigo, Y.X. Wang, C.C. Retsch, J. Opt. Soc. Am. A 17 (2000) 1732–1743.